UCSF

Title

NR2B Phosphorylation at Tyrosine 1472 Contributes to Brain Injury in a Rodent Model of Neonatal Hypoxia-Ischemia

Authors

Knox, Renatta

Brennan-Minnella, Angela M

Lu, Fuxin

et al.

NR2B phosphorylation at Tyrosine 1472 contributes to brain injury in a rodent model of neonatal hypoxia-ischemia

Renatta Knox, PhD[1,2,3], **Angela M. Brennan-Minnella, PhD**[4,5], **Fuxin Lu, MS**[1], **Diana Yang, BS**[1], **Takanobu Nakazawa, PhD**[6], **Tadashi Yamamoto, PhD**[6], **Raymond A. Swanson, MD**[4,5], **Donna M. Ferriero, MD**[1,2,4], and **Xiangning Jiang, PhD**[1]

[1]Department of Pediatrics, University of California, San Francisco, CA, 94158 USA

[2]Biomedical Sciences Graduate Program, University of California, San Francisco, CA, 94158 USA

[3]Medical Scientist Training Program, University of California, San Francisco, CA, 94158 USA

[4]Department of Neurology, University of California, San Francisco, CA, 94158 USA

[5]San Francisco Veterans Affairs Medical Center, University of California, San Francisco, CA, 94158 USA

[6] Division of Oncology, Institute of Medical Science, The University of Tokyo, Japan

Abstract

Background and Purpose—The NR2B subunit of the NMDA receptor (NMDAR) is phosphorylated by the Src family kinase Fyn in brain, with tyrosine (Y) 1472 as the major phosphorylation site. While Y1472 phosphrylation is important for synaptic plasticity, it is unknown whether it is involved in NMDAR-mediated excitotoxicity in neonatal brain hypoxiaischemia (HI). This study was designed to elucidate the specific role of Y1472 phosphorylation of NR2B in neonatal HI *in vivo* and in NMDA-mediated neuronal death *in vitro*.

Methods—Neonatal mice with a knock-in mutation of Y1472 to phenylalanine (YF-KI) and their wildtype (WT) littermates were subjected to HI using the Vannucci model. Brains were scored five days later for damage using cresyl violet and iron staining. Western blotting and immunoprecipitation were performed to determine NR2B tyrosine phosphorylation. Expression of NADPH oxidase subunits and superoxide production were measured in vivo. NMDA-induced calcium response, superoxide formation and cell death were evaluated in primary cortical neurons.

Results—After neonatal HI, YF-KI mice have reduced expression of NADPH oxidase subunit gp91[phox] and p47[phox] and superoxide production, lower activity of proteases implicated in necrotic and apoptotic cell death, and less brain damage compared to the WT mice. In vitro, YF-KI mutation diminishes superoxide generation in response to NMDA without effect on calcium accumulation; and inhibits NMDA and glutamate-induced cell death.

Corresponding author: Xiangning Jiang, Department of Pediatrics, University of California, San Francisco 675 Nelson Rising Lane Room 494, San Francisco, CA 94158 Tel: 415-502-7278 Fax: 415-502-7325 xiangning.jiang@ucsf.edu.

Disclosures: none

Conclusions—Upregulation of NR2B phosphorylation at Y1472 following neonatal HI is involved in superoxide-mediated oxidative stress and contributes to brain injury.

Keywords

NR2B; Fyn; tyrosine phosphorylation; neonatal brain; hypoxia-ischemia

Hypoxic-ischemic encephalopathy (HIE) remains a significant cause of death and disability in infants and children with few treatment options[1]. In our efforts to understand mechanisms and seek novel interventions, we found that Fyn, a Src family kinase, is associated with neuronal death following neonatal brain hypoxia-ischemia (HI) [2,3]. Fyn has many substrates in the brain, including the N-methyl-d-aspartate receptor (NMDAR) subunit NR2B, the predominant regulatory subunit in the developing brain. Fyn mediates NR2B phosphorylation on 7 tyrosine (Y) residues in its C-terminus, with Y1472 as the major site [4]. In adult rats subjected to brain ischemia, phosphorylation of NR2B at Y1472 (pY1472NR2B) is significantly and persistently upregulated [5]. Increase in pY1472NR2B is also reported after neonatal HI in postnatal day 7 (P7) rats [6] and mice [3]. However, the functional role of this specific modification and whether it is directly involved in brain injury are unknown.

Overall NR2B tyrosine phosphorylation and pY1472NR2B in murine brain are developmentally regulated with a gradual increase with age [4]. Y1472 phosphorylation is physiologically important because it is implicated in long-term potentiation and hippocampal synaptic plasticity [4,7]. At the molecular level, Y1472 phosphorylation prevents NMDAR internalization [8, 9], regulates NMDAR localization between synaptic and extrasynaptic membrane [8, 10] and affects NR2B downstream signaling transduction[8, 11].

NMDAR-mediated excitotoxicity and oxidative stress derived from superoxide (O_2^-) and related reactive oxygen species are important contributors in perinatal HI brain injury [1]. Excitotoxicity and oxidative stress are inextricably linked, as evidenced by studies showing that NMDAR-dependent neuronal death results partially from O_2^- produced largely by NADPH oxidase (NOX) and triggered by calcium influx via NR2B-containing NMDAR [12-14]. Neurons mainly express the NOX2 isoform, which contains the gp91^{phox} catalytic subunit and the p47^{phox} assembly subunit [15]. It is unknown whether NR2B tyrosine phosphorylation is coupled to NOX2 activation and superoxide formation in neonatal HI. Here, we determined the role of pY1472 NR2B using mice with a knock-in mutation of Y1472 to phenylalanine (YF-KI) [8].

Materials and Method

Animals

C57BL/6 YF-KI mice [8] were bred with wildtype (WT) mice to generate heterozygous animals at the Laboratory Animal Resource Center of University of California, San Francisco. The YF-KI mice are normal in brain anatomy and hippocampal LTP [8]. Heterozygous mice were crossed to generate WT and homozygous YF-KI littermates for experiments. Both sexes were used at P7.

Hypoxic-Ischemic Brain Injury

We adapted the Vannucci procedure for neonatal HI with ligation of the right common carotid artery and hypoxia for 40min [3]. Sham-operated animals received anesthesia and exposure of the artery without ligation or hypoxia.

Evaluation of Brain Injury

Five days after HI, brain damage was scored as described using brain sections stained with cresyl violet and Perl's iron stain [16].

Western Blotting (WB)

WB was performed with cortical tissue from sham-operated and the ipsilateral side of HI-injured animals. The following primary antibodies were used: NR2B (BD Transduction Laboratories, San Jose, CA), phospho-Y1252 NR2B and phospho-Y1336 NR2B (PhosphoSolutions, Aurora, CO), phospho-Y1472 NR2B and phospho-Y1070 NR2B (Cell Signaling Technology, Boston, MA), α-spectrin (Millipore, Billerica, MA), cleaved-caspase 3 (Cell Signaling), $p47^{phox}$ (Millipore), $gp91^{phox}$ (BD) and β-actin (Santa Cruz Biotechnology). Appropriate secondary HRP-conjugated antibodies were used and signal was visualized with enhanced chemiluminescence. Image J was used to measure the optical densities (OD) of blots on radiographic film after scanning.

Immunoprecipitation (IP)

IPs were performed to measure NR2B tyrosine phosphorylation [3]. 250μg protein was incubated with 4μg goat NR2B antibody (Santa Cruz) or 4μg normal goat IgG as negative control. Eluted immune complexes were applied for WB and probed with mouse 4G10 anti-phosphotyrosine (anti-pY) antibody (Millipore), then stripped and reprobed with mouse NR2B (BD) antibody. NR2B tyrosine phosphorylation was expressed as the OD ratio of phosphotyrosine (pY) to NR2B.

Detection of superoxide production in vivo

Dihydroethidium (dHEth) was used for superoxide measurement since it is oxidized by O_2^- to a fluorescent product[13]. dHEth (Invitrogen) was dissolved in DMSO at 10mg/ml and diluted to 1mg/ml in saline. It was injected intraperitoneally (5mg/kg) 3 hours before the mice were sacrificed at 24hr after HI. The mice were transcardially perfused with 4% PFA, the brains were dissected and post-fixed for 2hr followed by cryoprotection with 30% sucrose. Cryosections (12μm) were evaluated for oxidized dHEth (510/590 nm excitation/emission) and the fluorescence intensities were measured with Volocity software (Improvision). We analyzed three sections of each brain at the levels of injured cortical regions from 3 animals of each genotype. The results are presented as mean dHEth fluorescence intensity.

Immunofluorescent staining

Cryosections were treated with 2 N HCl for 10 min at 37°C and then with 0.5 M boric acid (pH 8.4) for 10 min at room temperature (RT). After blocking, cleaved-caspase-3 (Cell signaling) antibody in blocking solution with 2.5% goat serum was applied overnight at 4°C.

Secondary antibody (Alexa Fluor 568, Invitrogen) was applied for 1hr at RT and the nuclei were stained with DAPI. Images were captured with Zeiss Axiovert 100 microscope.

Primary Cortical Neuronal Culture

Cultures were prepared from the cortices of embryonic day 14 C57BL/6 mice and plated in poly-D-lysine coated 24-well plates or glass coverslips at a density of 1.65×10^6 cells/ml [13]. The neurons were maintained in NeuroBasal medium (Gibco) containing 5 mM glucose and used at day 10 in vitro (DIV10). Experiments were initiated by exchanging the medium with a balanced salt solution (BSS) containing 1.2 mM $CaCl_2$, 0.8 mM $MgSO_4$, 5.3 mM KCl, 0.4 mM KH_2PO_4, 137 mM $NaCl_2$, 0.3 mM $NaHPO_4$, 5 mM glucose, and 10 mM 1,4-piperazinediethanesulfonate (PIPES) buffer, pH 7.2. When NMDA or glutamate was added, the MgSO4 concentration in BSS was dropped to 0.4mM.

Calcium Imaging in primary neurons

To monitor changes in intracellular calcium, neurons were loaded for 30min with either 4μM Fura 4F-AM or Fura FF-AM (Molecular Probes, Grand Island, NY), washed once with BSS and allowed to recover for 20min at 37°C before addition of NMDA. The cells were exposed to 100μM NMDA for 30min and the images were acquired at either 10sec intervals for Fura4F or 30sec intervals for Fura FF, using excitation that alternated between 340nm and 380nm (emission>510nm). Calcium levels were expressed as changes in the 340/380nm signal ratio relative to baseline fluorescence (F/Fo) prior to stimulus, and quantified by integrating the change over baseline for the 30min observation period. Regions of interest were drawn around neuronal cell bodies. Measurements were made from 3 dissections with 2 coverslips per experiment, and 10-12 neurons per coverslip for a total of 60 - 72 neurons for each cell type.

Eth imaging of superoxide production in primary neurons

On DIV10, the medium was exchanged for BSS containing 5μM dHEth 10 - 20 minutes prior to addition of NMDA, and maintained throughout the duration of the experiment. The cells were exposed to 100μM NMDA for 30min and the images were acquired at 5-min intervals after adding NMDA using 510-550 nm excitation (> 580 nm emission) for dHEth. Superoxide production is presented as raw Eth fluorescence normalized to baseline levels prior to stimulus (F/F0).

Cell death measurement

Dead and live neurons were identified with fluorescence markers, propidium iodide and calcein-AM, which were added to the cultures 24 hours after NMDA exposure. In another set of experiment, the neurons were exposed to 100μM glutamate for 30min and cell death was determined 24hr thereafter. Live and dead neurons were counted in 3 randomly chosen fields in a minimum of 4 wells per plate.

Statistical Analysis

Brain injury scores are presented as median and interquartile range using Prism 4 nonparametric tests for analysis of variance (Kruskal-Wallis test). WB results are presented

as mean ± SD and were evaluated using SAS Wilcoxon-Mann-Whitney test. For cell culture experiments, one way analysis of variance (Tukeys post hoc test) was used and data are presented as mean ± SEM. Differences were considered significant at p<0.05.

Results

YF-KI mice have decreased brain injury following neonatal HI

YF-KI mice had decreased overall brain injury compared to WT animals [median = 16.25, range 11.5-19 in WT (n=18); median = 11, range 7.5-15 in YF-KI (n=23), WT vs. YF-KI p=0.034, Fig. 1A, B]. The cortex showed a significant decrease in brain injury in YF-KI mice compared to WT and the striatum showed a trend toward a significant decrease in brain injury (cortex p=0.013, striatum p=0.067, Fig. 1C). There were no differences in injury in the hippocampus (Fig.1C). There were no gender differences in WT or YF-KI mice (Fig. 1D).

YF-KI mice have less activity of calpain and caspase and less cell death at 24hr after HI

We assessed cell death by examining the activity of protease calpain and caspase-3 for their substrate α-spectrin. Calpain cleavage of α-spectrin produces a breakdown product (SBPD) of 150 and 145 kDa, while caspase cleavage of α-spectrin produces a 120-kDa fragment [3]. In WT mice, we found increased calpain and caspase activity, as measured by α-spectrin cleavage, at 1hr, 6hr and 24hr after injury. However, YF-KI mice did not differ from sham animals in calpain and caspase activity (Fig. 2A). Consistently, cleaved (activated)-caspase 3 protein levels were elevated in WT mice at 6hr and 24hr after injury, but not in YF-KI mice (Fig. 2A). Immunofluorecent staining showed markedly reduced cleaved-caspase-3 expression in the cortex of YF-KI mice compared to WT mice at 24hr after HI, in line with the extension of neurodegeneration as revealed by Fluoro-Jade B staining (Fig. 2B).

pY1472 affects NR2B tyrosine phosphorylation at specific sites

Next we determined the phosphorylation status of the NR2B subunit, as YF-KI mice are hypotyrosine phosphorylated in the amygdala [8]. The overall NR2B tyrosine phosphorylation was significantly decreased in the YF-KI mice in sham (reduced 70%) and HI-injured animals (Fig. 3A) confirming that Y1472 is the major tyrosine phosphorylated on NR2B. Regarding Fyn-mediated-other sites, pY1336NR2B and pY1252NR2B were increased after HI in WT mice (Fig. 3B). There was a small increase in pY1070, whose function has not been characterized [4], at 15min in WT animals (Fig. 3B).

Interestingly, YF-KI mice had a significant decrease in the expression of pY1070 (70% reduction), pY1252 (50% reduction) and pY1336 (20% reduction) in sham animals (p<0.05, WT vs. YF-KI, Fig. 3B). After HI, YF-KI mice had significantly less pY1252 at 15min, and less pY1070 for up to 6hrs compared to WT mice (Fig.3B). pY1336 had a trend toward decreased expression at 15min after HI in YF-KI mice compared to WT (p=0.083, Fig. 3B).

YF-KI mice have decreased superoxide generation following neonatal HI

To find out whether pY1472NR2B is functionally linked to superoxide generation, we measured superoxide following neonatal HI in YF-KI mice. At 24hr after HI, the oxidized

dHEth increased significantly only in the WT mice, but not in the YF-KI mice (Fig. 4A). Consistently, expression of p47^{phox}, the regulatory subunit required for NOX2 assembly, and gp91^{phox}, the catalytic subunit of the enzyme, peaked at 24hr in the WT mice, while in the YF-KI mice, there was substantially less p47^{phox} and gp91^{phox} expression at 24hr (p < 0.05, Fig. 4B).

YF-KI neurons have decreased superoxide production and less cell death in response to NMDA without differences in calcium response

NMDA treatment of WT neurons caused a significant increase in superoxide production, which was diminished substantially in YF-KI neurons (Mean peak Eth fluorescence; WT neurons 2.75 ± 0.09 vs. YF-KI neurons 1.34 ± 0.04. p < 0.001, Fig. 5A). Exposure of cortical neurons to NMDA resulted in a 1.6 fold increase in cell death relative to control (p < 0.01), and a 1.3 fold increase in response to glutamate (p < 0.05). However, cell death was remarkably reduced in YF-KI neurons when treated with NMDA or glutamate (p < 0.01, Fig. 5B). Interestingly, there was no difference in the increase of total intracellular Ca^{2+} ([Ca^{2+}]i) induced by NMDA between the WT and YF-KI neurons (mean peak fluorescence; WT neurons 1.55 ± 0.07 vs. YF-KI neurons 1.53 ± 0.057, p = 0.875, Fig. 6). YF-KI neurons showed a trend of slower [Ca^{2+}]i increase than WT neurons as assessed by Fura4F to accurately capture the initial transient (WT neurons took an average of 16.3min +/−1.31 to reach the peak fluorescence and YF-KI neurons took 18.3min +/- 0.94 to reach the peak), however, the difference was not statistically significant.

Discussion

We show for the first time that a mutation of NR2B tyrosine 1472 to phenylalanine (YF-KI) results in neuroprotection from cell death *in vivo* and *in vitro* implicating phosphorylation at this site in the pathogenesis of injury after hypoxia-ischemia. Our study identifies a previously unrecognized role of Y1472 phosphorylation of NR2B as a mediator of superoxide-associated oxidative damage during excitotoxicity, an effect that is independent of intracellular Ca2+ increase.

Studies have demonstrated that NOX2 is the main source of superoxide following NMDAR activation in cortical cultures and in hippocampus in vivo [12]. We found substantial superoxide production at 24hr after HI in the WT mice, with concomitant increase of key NOX2 subunit p47^{phox} and gp91^{phox}, which are required for NOX2 assembly and activation. This suggests that NOX2 might be associated with superoxide formation after neonatal HI, which is in agreement with another HI study in P7 rats [17], as well as an ibotenate-induced excitotoxic injury model in P5 mice [18]. However, we cannot rule out other O$_2^-$ sources including those produced in mitochondria or by other enzymes, such as xanthine oxidase and lipoxygenase. These increases are dramatically attenuated in the YF-KI mice *in vivo* and *in vitro* indicating that pY1472 NR2B regulates O$_1^-$ formation under hypoxia-ischemia and excitotoxicity. It should be noted that in vivo, both neurons [17] and microglia [18] could be the sources of NOX2 activation/ O$_2^-$ production. Microglia express functional NMDARs, including the NR2B subunit, in murine and human brain, although at significantly lower levels than the neurons. Activation of microglia NMDAR triggers inflammation and

neuronal cell death in the neonatal and mature brain [19]. We have not determined the cell-type specific distribution and expression of pY1472NR2B, so we cannot exclude the role of tyrosine phosphorylation of microglia NR2B in O_2^- formation and brain injury.

Our in vitro studies with pure cortical neurons clearly show that NR2B phosphorylation at Y1472 is essential for NMDA-induced superoxide formation and the resultant neuronal death. Calcium influx is required for NMDAR-mediated superoxide production[12], but our results indicate that calcium rise alone is not sufficient for this effect because YF-KI neurons have similar Ca^{2+} accumulation in response to NMDA but diminished superoxide generation compared to WT cells. Other Ca^{2+}-independent mechanisms linking Y1472 phosphorylation and NOX2 superoxide formation remain to be elucidated. Although phosphorylation of this site inhibits NMDAR internalization, there are no convincing data demonstrating a change in NR2B surface expression, in total NMDAR number at synapses, or in NMDAR subunit composition in the YF-KI mice [8]. Our Ca^{2+} influx results, together with data showing normal basic properties of synaptic transmission in YF-KI mice [8], suggest that the suppressed superoxide production does not result from reduced NMDAR activity in YF-KI neurons, but rather from altered downstream signaling or protein-protein interactions that mediate excitotoxicity.

Mutation of NR2B Y1472 does not cause compensation of tyrosine phosphoylation of other NR2B residues. On the contrary, in neonatal cortex, phosphorylation of at least 3 other Fyn-targeted residues on NR2B - Y1336, Y1252, and Y1070 was decreased in YF-KI mice. Two previous studies did not find changes in phosphorylation of Y1336 or Y1252 in YF-KI mice in amygdala or spinal cord [8, 11]. These discrepancies may be due to differences in brain regions studied or brain maturity. While the function of pY1070 and pY1252 is unknown, pY1336 mediates the interaction of NR2B with the p85 subunit of PI-3 kinase [20]. Additionally, YF-KI mice have decreased CaMKII and α-actinin associated with NR2B in amygdala [8]. Therefore, it is likely that changes in multiple tyrosine phosphorylation sites affects recruitment of proteins to the NR2B complex both in the naive state and after injury. How Y1472 phosphorylation regulates protein composition of NR2B complex merits further investigation. pY1472 NR2B is enriched in synaptic membranes in neonatal cortex [21] and increases following HI [3]. While there has been debate over the function of synaptic and extrasynaptic NMDARs in cell survival vs. death [22], several recent studies suggest a role for synaptic NMDAR in mediating NMDA-induced neurotoxicity [23] and hypoxic excitotoxic death [24]. Another report found that the C-terminal domain (CTD) of NR2B is linked to excitotoxic cell death [25].

Therefore, pY1472 is situated to affect cell death processes synaptically through its ability to modify proteins associated with the CTD of NR2B. Additionally, YF-KI mutation affects synaptic localization of NR1 and NR2B (shifting to the periphery of PSD and the perisynaptic regions) [8], but the consequences of this improper localization are unknown.

Taken together, we provide a mechanistic basis for injury after hypoxia-ischemia in the neonatal brain through increased NR2B tyrosine phosphorylation by Fyn. While pY1472NR2B is important for brain physiology, sustained upregulation may initiate downstream cell death signaling. Since neonatal brain is more vulnerable to free radical

injury than the mature brain[1], these findings could advance our understanding of mediators of oxidative damage in the immature brain and may have significant implications for neonatal HIE therapies.

Acknowledgments

References

1. Ferriero DM. Neonatal brain injury. N Engl J Med. 2004; 351:1985–1995. [PubMed: 15525724]

2. Jiang X, Mu D, Biran V, Faustino J, Chang S, Rincón CM, et al. Activated Src kinases interact with the N-methyl-D-aspartate receptor after neonatal brain ischemia. Ann Neurol. 2008; 63:632–641. [PubMed: 18384166]

3. Knox R, Zhao C, Miguel-Perez D, Wang S, Yuan J, Ferriero D, et al. Enhanced NMDA receptor tyrosine phosphorylation and increased brain injury following neonatal hypoxiaischemia in mice with neuronal Fyn overexpression. Neurobiol Dis. 2013; 51:113–119. [PubMed: 23127881]

4. Nakazawa T, Komai S, Tezuka T, Hisatsune C, Umemori H, Semba K, et al. Characterization of Fyn-mediated tyrosine phosphorylation sites on GluR epsilon 2 (NR2B) subunit of the N-methyl-D-aspartate receptor. J Biol Chem. 2001; 276:693–699. [PubMed: 11024032]

5. Zhang F, Guo A, Liu C, Comb M, Hu B. Phosphorylation and assembly of glutamate receptors after brain ischemia. Stroke. 2013; 44:170–176. [PubMed: 23212166]

6. Gurd JW, Bissoon N, Beesley PW, Nakazawa T, Yamamoto T, Vannucci SJ. Differential effects of hypoxia-ischemia on subunit expression and tyrosine phosphorylation of the NMDA receptor in 7- and 21-day-old rats. J Neurochem. 2002; 82:848–856. [PubMed: 12358790]

7. Rostas JA, Brent VA, Voss K, Errington ML, Bliss TV, Gurd JW. Enhanced tyrosine phosphorylation of the 2B subunit of the N-methyl-D-aspartate receptor in long-term potentiation. Proc Natl Acad Sci U S A. 1996; 93:10452–10456. [PubMed: 8816821]

8. Nakazawa T, Komai S, Watabe AM, Kiyama Y, Fukaya M, Arima-Yoshida F, et al. NR2B tyrosine phosphorylation modulates fear learning as well as amygdaloid synaptic plasticity. Embo J. 2006; 25:2867–2877. [PubMed: 16710293]

9. Prybylowski K, Chang K, Sans N, Kan L, Vicini S, Wenthold RJ. The synaptic localization of NR2B-containing NMDA receptors is controlled by interactions with PDZ proteins and AP-2. Neuron. 2005; 47:845–857. [PubMed: 16157279]

10. Goebel-Goody SM, Davies KD, Alvestad Linger RM, Freund RK, Browning MD. Phospho-regulation of synaptic and extrasynaptic N-methyl-d-aspartate receptors in adult hippocampal slices. Neuroscience. 2009; 158:1446–1459. [PubMed: 19041929]

11. Matsumura S, Kunori S, Mabuchi T, Katano T, Nakazawa T, Abe T, et al. Impairment of CaMKII activation and attenuation of neuropathic pain in mice lacking NR2B phosphorylated at Tyr1472. Eur J Neurosci. 2010; 32:798–810. [PubMed: 20722721]

12. Brennan AM, Suh SW, Won SJ, Narasimhan P, Kauppinen TM, Lee H, et al. NADPH oxidase is the primary source of superoxide induced by NMDA receptor activation. Nat Neurosci. 2009; 12:857–863. [PubMed: 19503084]

13. Girouard H, Wang G, Gallo EF, Anrather J, Zhou P, Pickel VM, et al. NMDA receptor activation increases free radical production through nitric oxide and NOX2. J Neurosci. 2009; 29:2545–2552. [PubMed: 19244529]

14. Brennan AM, Shen Y, Swanson RA. Phosphoinositide 3-kinase couples NMDA receptors to superoxide release in excitotoxic neuronal death. Cell Death Dis. 2013; 4:e580. [PubMed: 23559014]

15. Bedard K, Krause KH. The NOX family of ROS-generating NADPH oxidases: physiology and pathophysiology. Physiol Rev. 2007; 87:245–313. [PubMed: 17237347]

16. Sheldon RA, Sedik C, Ferriero DM. Strain-related brain injury in neonatal mice subjected to hypoxia–ischemia. Brain Res. 1998; 810:114–122. [PubMed: 9813271]

17. Lu Q, Wainwright MS, Harris VA, Aggarwal S, Hou Y, Rau T, et al. Increased NADPH oxidase-derived superoxide is involved in the neuronal cell death induced by hypoxiaischemia in neonatal hippocampal slice cultures. Free Radic Biol Med. 2012; 53:1139–1151. [PubMed: 22728269]

18. Doverhag C, Keller M, Karlsson A, Hedtjarn M, Nilsson U, Kapeller E, et al. Pharmacological and genetic inhibition of NADPH oxidase does not reduce brain damage in different models of perinatal brain injury in newborn mice. Neurobiol Dis. 2008; 31:133–44. [PubMed: 18571099]

19. Kaindl AM, Degos V, Peineau S, Gouadon E, Chhor V, Loron G, et al. Activation of microglial N-methyl-D-aspartate receptors triggers inflammation and neuronal cell death in the developing and mature brain. Ann Neurol. 2012; 72:536–49. [PubMed: 23109148]

20. Hisatsune C, Umemori H, Mishina M, Yamamoto T. Phosphorylation-dependent interaction of the N-methyl-D-aspartate receptor epsilon 2 subunit with phosphatidylinositol 3-kinase. Genes Cells. 1999; 4:657–666. [PubMed: 10620012]

21. Jiang X, Knox R, Pathipati P, Ferriero D. Developmental localization of NMDA receptors, Src and MAP kinases in mouse brain. Neurosci Lett. 2011; 503:215–219. [PubMed: 21896318]

22. Hardingham GE, Bading H. Synaptic versus extrasynaptic NMDA receptor signalling: implications for neurodegenerative disorders. Nat Rev Neurosci. 2010; 11:682–696. [PubMed: 20842175]

23. Papouin T, Ladépêche L, Ruel J, Sacchi S, Labasque M, Hanini M, et al. Synaptic and Extrasynaptic NMDA Receptors Are Gated by Different Endogenous Coagonists. Cell. 2012; 150:633–646. [PubMed: 22863013]

24. Wroge CM, Hogins J, Eisenman L, Mennerick S. Synaptic NMDA receptors mediate hypoxic excitotoxic death. J Neurosci. 2012; 32:6732–6742. [PubMed: 22573696]

25. Martel MA, Ryan TJ, Bell KF, Fowler JH, McMahon A, Al-Mubarak B, et al. The subtype of GluN2 C-terminal domain determines the response to excitotoxic insults. Neuron. 2012; 74:543–556. [PubMed: 22578505]
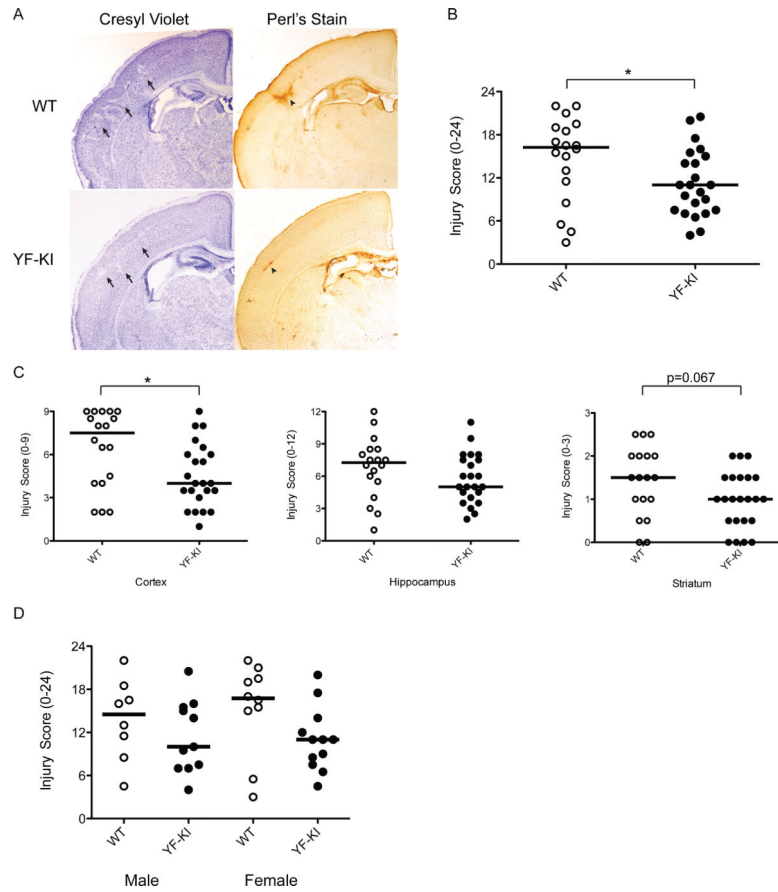
Figure 1. YF-KI mice have decreased brain injury following neonatal HI
A) Brain sections were stained with Cresyl violet and Perl's iron stain. Arrows indicate patches of cell loss and arrowheads show iron accumulation in similar injured areas. B) Composite injury score and D) composite injury score by sex. C) Regional injury scores in cortex, hippocampus and striatum. The horizontal lines represent the median. *p<0.05.
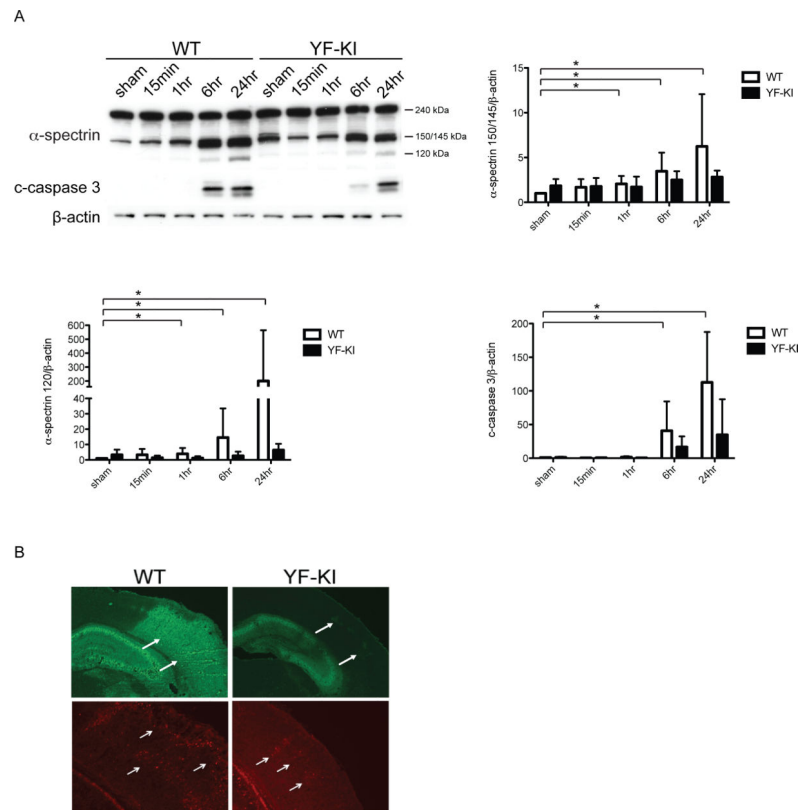
Figure 2. YF-KI mice have less activity of calpain and caspase and less cell death at 24hr after HI

A) Western blots using anti-α-spectrin, cleaved-caspase 3 and β-actin with cortical lysates from sham and HI animals. Expression of SBDP 150/145; SBDP 120; and cleaved-caspase 3 was normalized to β-actin. Data (n=4) was normalized to WT sham values (*p<0.05). B) Representative images of brain sections stained with Fluro-Jade (green) and cleaved caspase-3 (red) at 24hr after HI.
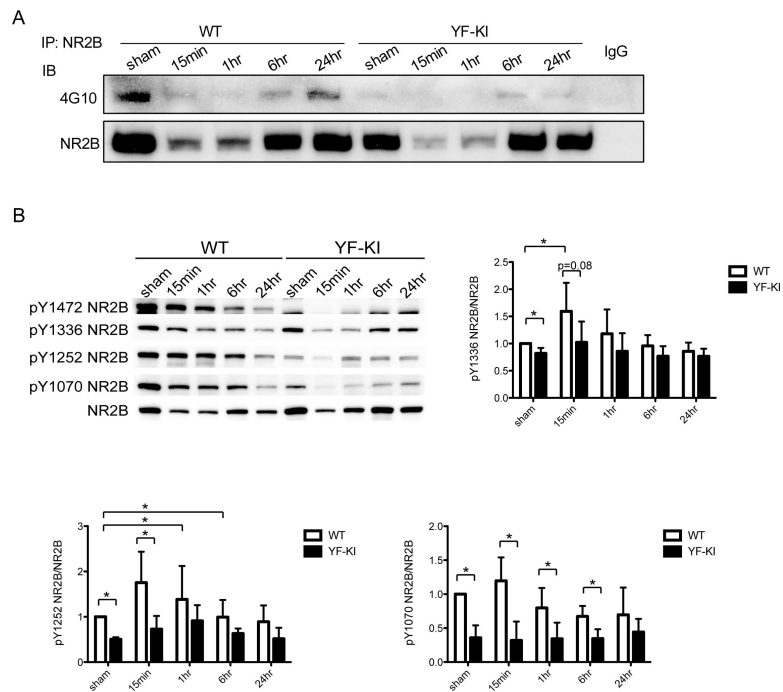
Figure 3. Y1472 phosphorylation affects overall NR2B tyrosine phosphorylation and phosphorylation at specific residues

A) IP with goat NR2B antibody followed by immunoblotting (IB) with anti-phosphotyrosine (4G10) antibody. The membrane was re-probed with mouse NR2B antibody. IP with normal goat IgG served as negative control. B) Western blots using antibodies against NR2B phosphorylated at specific sites. The OD values of NR2B-specific sites were normalized to those of NR2B. Data was normalized to WT sham values (n=4). *p<0.05.
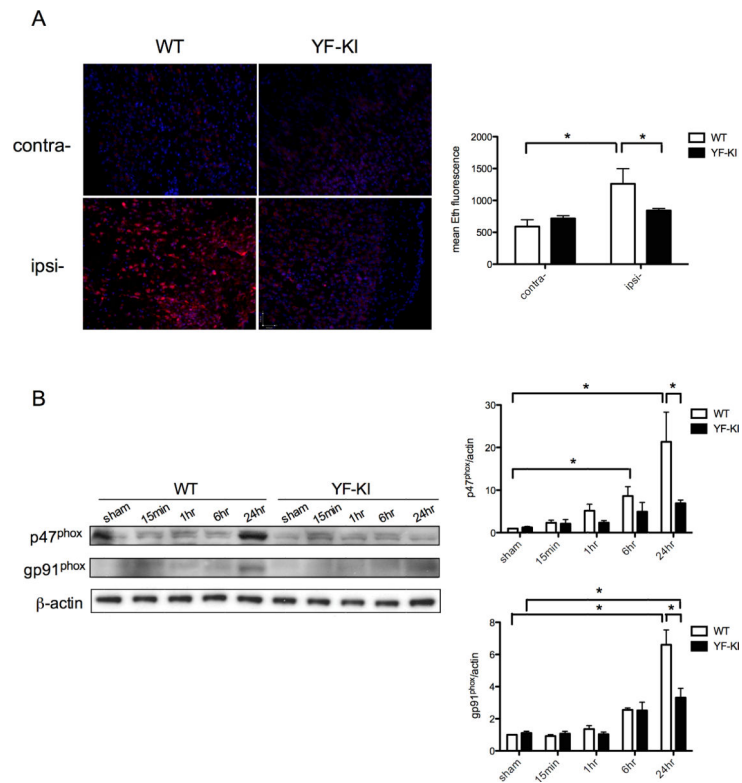
Figure 4. YF-KI mice have reduced superoxide generation and decreased expression of NOX2 component p47^{phox} and gp91^{phox} following neonatal HI

A) Representative dHEth images from contralateral (contra-) and ipsilateral (ipsi-) cortex at 24hr after HI (scale bar = 40μm). Quantification of mean oxidized Eth fluorescence (right).

B) Western blots using antibodies against NOX2 subunit p47^{phox} and gp91^{phox}. *p< 0.05.
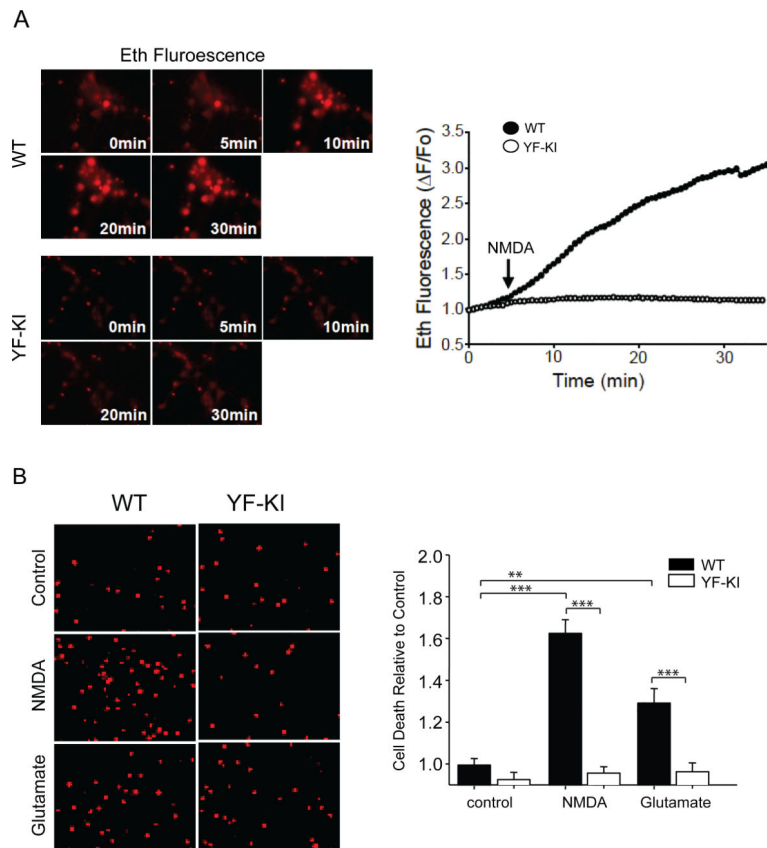
Figure 5. YF-KI neurons have decreased superoxide production in response to NMDA and are protected from NMDA- and glutamate-induced cell death

A) Eth fluorescence before NMDA application (0 minutes), at the time of NMDA addition (5 minutes) and then at 5 minute intervals in WT or YF-KI neurons. Representative Eth fluorescence transients (right) showed superoxide production in WT neurons (black circles) following NMDA application (arrow) compared to YF-KI neurons (open circles). $p < 0.001$. B) Propidium iodide labeled dead neurons 24 hours after NMDA or glutamate treatment in WT or YF-KI neurons. ** $p < 0.05$, *** $p < 0.01$, n = 3.
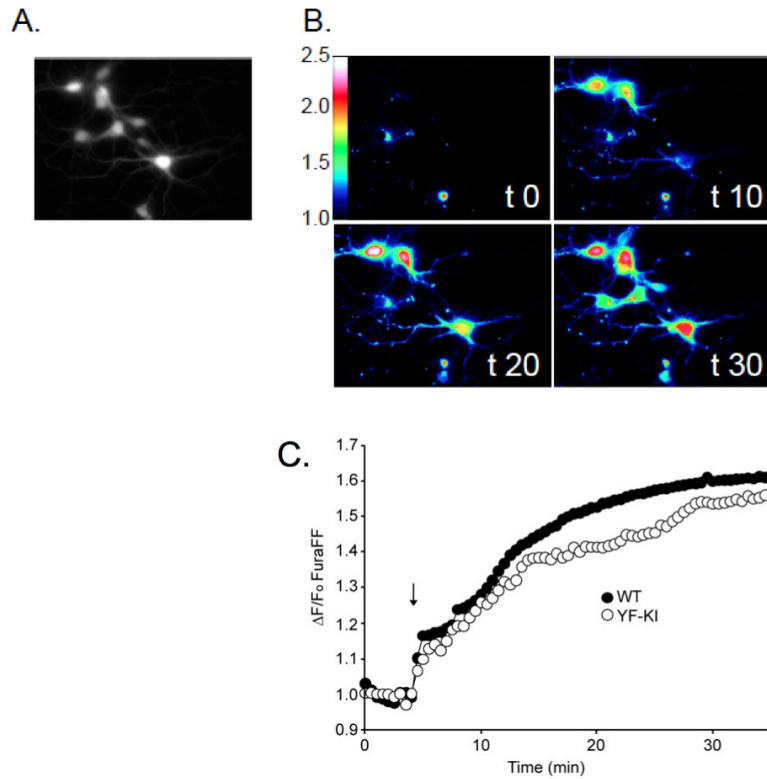
Figure 6. YF-KI neurons have similar increase in total intracellular calcium in response to NMDA

A) Grey scale image of YF-KI neurons loaded with Fura FF (4uM) before NMDA treatment B) showed a significant increase in calcium. Panels show color-coded images of this calcium increase relative to baseline fluorescence (F/Fo) at 10, 20 and 30mins after NMDA application. C) Representative traces showed that increase in calcium following application of NMDA (arrow) is not different between WT (closed circles) and YF-KI (open circles) neurons. (n=3, for each experiment, measurements were made in two coverslips with 10-12 neurons per coverslip for a total of 60-72 neurons each group).